Lanthanide(III) Squarates
1. Five Families of Compounds Obtained from Aqueous Solutions in an Open System. Crystal Structure and Thermal Behaviour

JEAN-FRANCOIS PETIT, ALAIN GLEIZES and JEAN-CHRISTIAN TROMBE*

Laboratoire de Chimie de Coordination du C.N.R.S., Unité Propre no. 8241 liée par conventions à l'Université Paul Sabatier et à l'Institut National Polytechnique de Toulouse, 205 route de Narbonne, 31077 Toulouse Cédex (France)

(Received March 3, 1989; revised July 31, 1989)

Abstract

Five families of hydrated lanthanide(III) squarates of respective formulae $Ln_2(H_2O)_{11}(C_4O_4)_3 \cdot 2H_2O$ (1-Ln), $[Ln(H_2O)_4]_2(C_4O_4)_3$ (2-Ln), $H[Ln(H_2O)_x(C_4O_4)_2] \cdot yH_2O$ $(x+y=6)$ (1(H)-Ln), $Ln(H_2O)_6(C_4O_4)(HC_4O_4) \cdot H_2O$ (2(H)-Ln), $H[Ln(H_2O)_6(C_4O_4)_2]$ (3(H)-Ln), were prepared by reaction of aqueous solutions of lanthanide salts and squaric acid or squarate anion. The formula of the compound produced depends on the Ln(III) cation radius and conditions of preparation. The crystal structures of the following representative compounds were determined by X-ray single crystal techniques. 1-Pr: monoclinic, space group $P2/c$, $a = 9.687(1)$, $b = 7.632(1)$, $c = 16.423(1)$ Å, $\beta = 89.95(1)°$, $V = 1214$ Å^3, $Z = 2$. 2-Eu: monoclinic, space group Pc, $a = 11.937(2)$, $b = 8.205(1)$, $c = 10.106(2)$ Å, $\beta = 96.04(1)°$, $V = 984$ Å^3, $Z = 2$. 2(H)-Eu: monoclinic, space group Cc, $a = 15.263(2)$, $b = 14.898(1)$, $c = 6.354(1)$ Å, $\beta = 92.24(1)°$, $V = 1444$ Å^3, $Z = 4$. 3(H)-Yb: monoclinic, space group $C2/c$, $a = 10.272(1)$, $b = 12.450(1)$, $c = 11.760(1)$ Å, $\beta = 110.78(1)°$, $V = 1406$ Å^3, $Z = 4$. None of the 1(H)-Ln compounds gave crystals suitable for an X-ray structure determination. The squarate anion behaves like a uni- or a plurimonodentate ligand. 1-Ln has a double-chained structure; 2-Ln has a double-layered structure. 2(H)-Ln and 3(H)-Ln are made of discrete mononuclear entities. In 2(H)-Ln, the presence of a monohydrogenosquarate ligand is clearly established, while in 3(H)-Ln, the proton is likely to be shared by two neighbouring squarate ligands. Both thermal gravimetry and thermal differential analyses were carried out on compounds of the five families in the temperature range 20–800 °C, in a 50% He–50% O_2 atmosphere. The existence of anhydrous squarates stable over wide ranges of temperature was shown. The results are compared with those of the well known lanthanide oxalates and those of another work that do not match ours.

*Author to whom correspondence should be addressed.

Introduction

We have undertaken a systematic study of the lanthanide(III) squarates as obtained from aqueous solutions, with the aim of comparing their variety of phases, structural features and thermal behaviours with those of oxalates that had been extensively studied. When this work was initiated in 1985 as a major part of the Thèse d'Université of one of us [1], the only published work about lanthanide squarates dealt with the thermodynamics of the formation of complexes of the squaric acid with lanthanides in water [2, 3]. Two papers by Brzyska and Ozga [4, 5] appeared in 1987 that partially covered our field of research. When we could read these papers our investigation was already well developed, as for the main topics of the Polish papers, viz. characterization and thermal analysis of several phases. By that time, we had also carried out several crystal structure determinations which supported our results versus some discrepancies in the Polish articles.

The compounds produced may be divided into two categories depending on the procedure of preparation. The present paper deals with compounds obtained in an open system, i.e. by evaporating aqueous solutions. Compounds prepared in a closed system, namely a sealed pyrex glass tube or a steel container, will be described in a following paper [6].

Experimental

Syntheses and Characterization

The general scheme of preparation consisted in reacting a solution of squaric acid with a solution of a lanthanide salt (chloride or nitrate) at 40–50 °C under stirring during a few minutes, and then allowing it to cool down and evaporate. After a few hours or days, single crystals or microcrystal powders separated and were washed with water and air dried. All had the expected colour or absence

0020-1693/90/$3.50

TABLE 1. Formulae of the lanthanide squarates prepared under conditions A, B or C described in 'Experimental'

A. Formulae and types of structure according to the stoichiometry

General formula	Type	Composition
$Ln_2(H_2O)_x(C_4O_4)_3 \cdot yH_2O$	**1**-Ln	$x = 11$ $y = 2$
	2-Ln	$x = 8$ $y = 0$
$Ln(H_2O)_x(C_4O_4)_2H \cdot yH_2O$	**1**(H)-Ln	$x + y = 6$
	2(H)-Ln	$x = 6$ $y = 1$
	3(H)-Ln	$x = 6$ $y = 0$

B. Types of structure according to the experimental conditions and lanthanides

Ln	La	Ce	Pr	Nd	Sm	Eu	Gd	Tb	Dy	Ho	Y	Er	Yb	Lu
Conditions														
A		**1**				**2**					**2**(H)			
B		**1**							**2**					
C	**1**		**1**(H)		**2**				**2**(H)				**3**(H)	

of colour corresponding to their Ln(III) cation, except the europium derivatives that had the yellow coloration of Eu(II) salts. Three sets of experimental conditions were tested.

Conditions A: mixture of equimolecular diluted solutions (0.3 mmol/10 ml)

Conditions B: as A + pH adjusted to 6–7

Conditions C: mixture of equimolecular less diluted solutions (3 mmol/10 ml)

As a general remark, crystals grown from an acid medium were more developed than when grown from a neutral medium and the heavier the lanthanide, the easier the crystal growth.

The formulae of the different compounds obtained are given in Table 1 with respect to the relevant experimental conditions and lanthanides. The classification into families **1**-Ln, 2-Ln, **1**(H)-Ln, 2(H)-Ln, **3**(H)-Ln, is based on similarity of X-ray powder patterns and stoichiometry. Elemental analyses are reported in Table 2 (the two **3**(H)-Ln compounds were not submitted to elemental analysis).

Thermal Analyses

Thermogravimetry analyses were carried out on a SETARAM B85 microbalance controlled by a SETARAM TGC85 programmer. Thermal decompositions were carried out on 20–30 mg samples in a mixed (He, O_2) flow with a heating rate of 5°/min.

A SETARAM M5 microanalyser was used for differential thermal analyses. In a typical procedure, a 10 mg sample was placed in a platinum crucible and heated in static air at a heating rate of 5°/min with α-Al_2O_3 as a standard for temperature and DTA measurements.

TABLE 2. Elemental analyses for the compounds prepared

Compound	Found (%)			Calculated (%)		
	Ln	C	H	Ln	C	H
1-La	33.4	17.4	3.1	32.77	16.98	3.07
1-Ce	32.5	16.9	3.2	32.96	16.94	3.06
1-Pr	32.4	17.1	3.2	33.08	16.90	3.05
1-Nd	34.0	16.8	3.0	33.60	16.77	3.03
2-Sm	39.1	18.4	2.0	38.52	18.44	2.05
2-Eu	38.9	18.6	2.3	38.77	18.37	2.04
2-Gd		18.2	2.2		18.12	2.01
2-Tb		18.0	2.1		18.05	2.00
2-Dy	38.2	17.6	2.1	40.37	17.89	1.99
2-Ho		17.7	2.1		17.78	1.98
2-Er		17.6	2.0		17.68	1.96
2-Yb		17.3	2.0		17.43	1.94
2-Lu		17.2	1.9		17.35	1.93
1(H)-Ce	28.7	20.0	2.7	29.62	20.29	2.75
1(H)-Pr	28.6	20.2	2.6	29.73	20.26	2.74
1(H)-Nd	31.4	19.8	2.7	30.22	20.12	2.72
2(H)-Eu		19.0	2.9		19.09	2.98
2(H)-Gd		18.8	3.1		18.89	2.95
2(H)-Tb		18.7	3.1		18.83	2.94
2(H)-Dy	31.7	18.7	2.9	31.64	18.69	2.92
2(H)-Ho	33.0	18.8	2.7	31.97	18.61	2.91
2(H)-Er		18.4	3.0		18.52	2.89
2(H)-Yb	32.9	18.4	2.9	33.02	18.32	2.86
2(H)-Lu		18.1	2.9		18.25	2.85

Crystal Structure Determinations

Single crystals of **1**-Pr, **2**-Eu, **2**(H)-Eu and **3**(H)-Yb were mounted on an Enraf-Nonius CAD 4 diffractometer. Orientation matrices and accurate cell constants were derived from least-squares refinements of the setting angles of 25 reflections. Diffracted intensities were measured at room temperature under conditions reported in Table 3. Standard reflections showed no abnormal trend. The data were corrected for Lorentz polarization. The data of **2**-Eu and **2**(H)-Eu were also corrected for absorption.

Structure determinations were carried out using Patterson and Fourier map techniques and full-matrix least-squares refinement techniques on a DEC VAX 11-730 computer using programs listed in ref. 7. Atomic scattering factors and anomalous terms are those of Cromer and Waber [8]. Throughout the refinement, the minimized function was $\Sigma w(F_o - |F_c|)^2$ where F_o and $|F_c|$ are the observed and calculated structure factor amplitudes. Weighting schemes and reliability factors are given in Table 3.

The H atoms which were located from difference Fourier maps were introduced in the last cycles of refinement as fixed contributors with isotropic thermal parameters equal to those of atoms to which they were attached.

$Pr_2(H_2O)_{11}(C_4O_4)_3 \cdot 2H_2O$ (1-Pr)

The systematic absences of reflections *h0l* with odd *l* were consistent with space group *P2/c* (centrosymmetric) and *Pc* (non-centrosymmetric). The structure refinement was started using *P2/c*. The four expected Pr atoms, four of the six expected squarate groups and the water molecules were located easily on general positions ($R = 0.08$, $R_w = 0.10$, with anisotropic thermal parameters for Pr only). The missing squarate groups (one-half per assymmetric unit) did not show up clearly in the subsequent difference Fourier map. This suggested that the actual space group should be *Pc*. Any attempt to refine the structure in *Pc* failed and, back to *P2/c*, the possibility of a disorder was considered. A series of peaks matching quite well a possible squarate C-square ring was found at such a proximity of the twofold axis that they were too close to their equivalent to have a 100% occupancy. Moreover three of the expected corresponding oxygen positions were already fully occupied by water

TABLE 3. Experimental crystallographic data for **1**-Pr, **2**-Eu, **2**(H)-Eu and **3**(H)-Yb

	1-Pr	**2**-Eu	**2**(H)-Eu	3(H)-Yb
Crystal data				
Crystal system	monoclinic	monoclinic	monoclinic	monoclinic
Space group	*P2/c* (see text)	*Pc*	*Cc*	*C2/c*
a (Å)	9.687(1)	11.937(2)	15.263(2)	10.272(1)
b (Å)	7.632(1)	8.205(1)	14.898(1)	12.450(1)
c (Å)	16.423(1)	10.106(2)	6.354(1)	11.760(1)
β (°)	89.95(1)	96.04(1)	92.24(1)	110.78(1)
V (Å^3)	1214	984	1444	1406
Z	2	2	4	4
Molecular weight	834.1	784.2	503.2	506.2
ρ_{cal} (g cm^3)	2.28	2.65	2.32	2.39
Data collection				
Scan mode	θ–2θ	ω	θ–θ	θ–$2/3\theta$
Take-off angle (°)	3	3	3	3.25
Max. Bragg angle (°)	30	29	35	35
Scan speed[a]				
SIGPRE[a]	0.80	0.80	0.75	0.67
SIGMA[a]	0.018	0.018	0.018	0.018
VPRE (°/min)[a]	10	6.67	10	10
T_{max} (s)[a]	80	90	50	45
Structure refinement				
Reflections collected	3994	2910	3179	6693
Reflections used	2511 ($I > 3\sigma(I)$)	2018 ($I > 2\sigma(I)$)	2950 ($I > 3\sigma(I)$)	2278 ($I > 3\sigma(I)$)
Weighting w^{-1} =	$\sigma^2(F_o) + (0.02F_o)^2 + 1$	$\sigma^2(F_o) + (0.01F_o)^2 + 3$	$\sigma^2(F_o) + (0.025F_o)^2 + 1$	$\sigma^2(I) + (0.05I)^2$
$R = \Sigma(\|F_o - F_c\|)/\Sigma F_o$	0.027	0.027	0.022	0.024
$R_w = (\Sigma w(F_o - F_c)^2/\Sigma F_o^2)^{1/2}$	0.030	0.046	0.029	0.033

[a]For definition of parameters see ref. 9.

oxygen atoms and the fourth one covered the equivalent position of the nearest C peak to the twofold axis. The latter position was attributed to a theoretical (C + O)/2 mixed atom with full site occupancy. The three supposed C atoms were introduced with 50% occupancies which implied that they were attached to oxygen atoms which were 50% from squarate and 50% from water. The convergence was rapidly achieved and the r.m.s. amplitudes of thermal vibration of the three 'half-water, half-squarate' oxygen atoms did not show strong anisotropy, thus indicating that the two kinds of atoms occupied very close, if not coinciding, positions.

Several water H atoms could be located. In the last cycle of refinement the largest (variable shift)/(e.s.d.) ratio was equal to 0.01 and the reliability factors stabilized at $R = 0.027$ and $R_w = 0.033$ for 2511 observations with $I > 3\sigma(I)$ and 190 variables. The error in an observation of unit weight was 0.99 e. The final difference Fourier map did not give significant features. The atomic coordinates are given in Table 4.

TABLE 4. Atomic positions for **1**-Pr

Atom	*x*	*y*	*z*
Pr	0.21071(3)	0.18030(3)	−0.09963(3)
$O_w(1)$	0.1708(4)	−0.0335(5)	0.0117(2)
$O_w(2)$	0.2119(4)	0.1724(5)	−0.2578(2)
$O_w(3)$	0.3817(4)	0.2339(6)	0.0108(8)
$O_w(4)$	0.4587(4)	0.1828(5)	−0.1554(2)
O_w	0.3369(5)	0.6672(5)	0.0198(2)
O(11)	−0.2932(5)	0.5225(5)	0.1254(2)
O(21)	−0.2974(4)	0.1068(4)	0.1336(2)
O(31)	−0.3520(4)	0.1181(5)	0.3280(2)
O(41)	−0.3452(5)	0.5441(5)	0.3206(2)
$O_{sw}(1)$	−0.0023(4)	0.0027(5)	0.1453(2)
$O_{sw}(2)$	0.0812(5)	0.3391(5)	0.0159(2)
$O_{sw}(3)$	−0.0134(4)	0.6368(5)	0.1525(3)
O(C)	0.0091(5)	0.3144(6)	0.2127(2)
C(1)	0.0088(8)	0.186(1)	0.1444(5)
C(2)	0.0326(8)	0.324(1)	0.0838(5)
C(3)	−0.0036(9)	0.458(1)	0.1458(5)
C(11)	−0.3129(6)	0.4138(6)	0.1818(3)
C(21)	−0.3139(5)	0.2239(5)	0.1850(3)
C(31)	−0.3396(5)	0.2304(6)	0.2735(3)
C(41)	−0.3359(6)	0.4228(6)	0.2695(3)
H(11)	0.139	−0.041	0.059
H(21)	0.221	−0.125	0.008
H(12)	0.221	0.082	−0.289
H(22)	0.250	0.250	−0.289
H(13)	0.391	0.207	0.061
H(23)	0.445	0.250	0.010
H(14)	0.500	0.043	−0.145
H(24)	0.500	0.250	−0.178
H(1)	0.332	0.584	−0.010
H(2)	0.332	0.584	0.059

$[Eu(H_2O)_4]_2(C_4O_4)_3$ (2-Eu)

The systematic absences of reflections *h*0*l* with odd *l* indicated $P2/c$ or Pc as possible centrosymmetric and non-centrosymmetric space groups. The structure was first refined in $P2/c$. One Eu atom, one squarate entity and six oxygen atoms were easily located and refined ($R = 0.09$, $R_w = 0.14$; anisotropic Eu). The missing squarate entity (one-half per asymmetric unit) could not be located on the subsequent difference Fourier map where some peaks suggested that the structure should be non-centrosymmetric. The structure refinement was started again in space group Pc. The missing atoms were clearly located. However the parameters of pseudocentrosymmetrically related but chemically non-equivalent oxygen atoms appeared to be strongly correlated. Then, it was necessary to refine in two blocks. Eu and O atoms were refined anisotropically and C atoms isotropically. After several cycles of refinement using a dampening coefficient which was progressively increased to 1, convergence was achieved and the process was stopped when the highest (variable shift)/(e.s.d.) ratio was 0.70. The reliability factors stabilized at $R = 0.027$ and $R_w = 0.046$, for 280 variables and 2018 observations having $I > 2\sigma(I)$. The error in an observation of unit weight was 1.09 e. The final difference Fourier map did not give significant features. The atomic coordinates are listed in Table 5.

TABLE 5. Atomic positions for **2**-Eu

Atom	*x*	*y*	*z*
Eu(1)	0	0.75571(5)	0
Eu(2)	0.50827(5)	0.74862(6)	0.23501(5)
$O_w(11)$	−0.0581(8)	0.984(1)	−0.1402(8)
$O_w(21)$	−0.1775(8)	0.852(1)	0.065(1)
$O_w(31)$	0.007(1)	0.676(1)	0.2386(8)
$O_w(41)$	0.1766(9)	0.836(1)	−0.059(1)
$O_w(12)$	0.3263(8)	0.663(1)	0.282(1)
$O_w(22)$	0.5591(9)	0.520(1)	0.3653(9)
$O_w(32)$	0.500(1)	0.828(1)	0.010(1)
$O_w(42)$	−0.3481(9)	0.962(1)	0.267(1)
O(11)	0.1119(9)	0.489(1)	0.524(1)
O(21)	0.1869(8)	0.831(1)	0.4125(8)
O(31)	0.0413(7)	1.006(1)	0.6396(8)
O(41)	0.0049(8)	0.655(1)	0.7670(9)
O(12)	0.4482(7)	0.4820(9)	0.5871(7)
O(22)	0.3244(9)	0.658(1)	0.8078(9)
O(32)	0.3960(9)	1.011(1)	0.714(1)
O(42)	0.4984(8)	0.838(1)	0.4591(8)
O(13)	0.6572(9)	0.257(1)	0.251(1)
O(23)	0.802(1)	0.170(1)	0.006(1)
O(33)	0.8696(9)	0.550(1)	−0.038(1)
O(43)	0.6820(9)	0.640(1)	0.170(1)
C(11)	0.102(1)	0.627(1)	0.558(1)
C(21)	0.1375(8)	0.790(1)	0.514(1)
C(31)	0.075(1)	0.863(1)	0.618(1)

(continued)

TABLE 5. *(continued)*

Atom	x	y	z
C(41)	0.064(1)	0.702(1)	0.676(1)
C(12)	0.430(1)	0.626(1)	0.615(1)
C(22)	0.374(1)	0.708(2)	0.716(1)
C(32)	0.400(1)	0.866(1)	0.663(1)
C(42)	0.460(1)	0.782(1)	0.564(1)
C(13)	0.707(1)	0.348(2)	0.173(1)
C(23)	0.784(1)	0.297(2)	0.066(1)
C(33)	0.806(1)	0.458(2)	0.049(1)
C(43)	0.726(1)	0.515(2)	0.139(1)
H(111)	−0.033	0.999	−0.220
H(211)	−0.119	1.082	−0.109
H(121)	−0.228	0.861	−0.001
H(221)	−0.207	0.834	0.125
H(131)	−0.001	0.584	0.249
H(231)	−0.068	0.709	0.249
H(141)	0.192	0.793	−0.138
H(241)	0.192	0.918	−0.055
H(112)	0.272	0.749	0.313
H(212)	0.293	0.584	0.334
H(122)	0.606	0.529	0.418
H(222)	0.481	0.473	0.418
H(132)	0.484	0.918	−0.027
H(232)	0.563	0.779	−0.020
H(142)	−0.344	1.082	−0.721
H(242)	−0.308	0.918	0.307

$Eu(H_2O)_6(C_4O_4)(HC_4O_4)\cdot H_2O$ (2(H)-Eu)

The systematic absence of reflexions *hkl* with $h+k$ odd and *h0l* with $h+l$ odd, indicated $C2/c$ or Cc as possible space groups. The structure was first refined using $C2/c$. The atoms located corresponded to anionic units $[Eu(H_2O)_6(C_4O_4)_2\cdot\frac{1}{2}H_2O]^-$ having crystallographically imposed point symmetry 2, with a statistical distribution of the non-coordinated water molecules in general positions 8(f) nearby the twofold axis, close enough (2.48(1) Å) to one or the other squarate to be possibly H-bonded to it. Since these general positions were also close to inversion centres, the site occupation could not be higher than 25%, which meant that only half the anionic units accommodated a non-coordinated water molecule. Refining the non-H atoms anisotropically, introducing the H atoms as fixed contributors, gave reliability factors stabilized at $R = 0.031$, $R_w = 0.061$, for 115 variables and 2950 observations $I > 3\sigma(I)$.

The rather tricky resulting structure and the unusual gap between R and R_w were good reasons to redetermine the structure in Cc space group. A more plausible structure showed up, made of dissymmetric $[Eu(H_2O)_6(C_4O_4)_2\cdot H_2O]^-$ entities, no more calling out a disorder to locate the non-coordinated water molecule. Moreover, the 'proton counterion' could be located (see description of the structure), which was not the case in $C2/c$. Using the refinement conditions described above, the reliability factors stabilized at $R = 0.022$ and $R_w = 0.029$ for 216 variables. In the last cycle of refinement, the highest (variable shift)/(e.s.d.) ratio was 0.03, and the error in an observation of unit weight was 0.96 electron. The final difference Fourier map did not show significant features. The atomic coordinates are listed in Table 6.

TABLE 6. Atomic positions for **2**(H)-Eu

Atom	x	y	z
Eu	0	0.22188(1)	1/4
$O_w(1)$	0.1423(2)	0.1526(2)	0.2613(7)
$O_w(2)$	0.0628(3)	0.2828(3)	0.5806(7)
$O_w(3)$	−0.0016(3)	0.1009(3)	0.4980(7)
$O_w(4)$	−0.0035(4)	0.5310(5)	0.394(1)
O(1)	−0.0897(2)	0.3388(2)	0.3640(6)
O(2)	−0.2833(2)	0.2602(2)	0.2537(6)
O(3)	−0.3600(2)	0.4658(2)	0.2529(5)
O(4)	−0.1651(2)	0.5420(2)	0.3354(6)
C(1)	−0.1644(2)	0.3718(2)	0.3325(5)
C(2)	−0.2526(2)	0.3371(2)	0.2858(6)
C(3)	−0.2863(2)	0.4298(2)	0.2806(6)
C(4)	−0.1972(2)	0.4635(2)	0.3228(5)
H(11)	0.152	0.094	0.256
H(21)	0.195	0.180	0.244
H(12)	0.111	0.264	0.635
H(22)	0.070	0.365	0.563
H(13)	0.043	0.078	0.563
H(23)	−0.055	0.078	0.537
H(14)	0.014	0.584	0.463
H(24)	0.014	0.500	0.291
H(4)	−0.111	0.533	0.414

TABLE 7. Atomic positions for **3**(H)-Yb

Atom	x	y	z
Yb	0	0.34574(1)	1/4
$O_w(1)$	−0.1505(2)	0.4910(2)	0.2018(2)
$O_w(2)$	−0.0373(2)	0.4001(2)	0.0515(2)
$O_w(3)$	0.0986(2)	0.2054(2)	0.3757(2)
O(1)	0.1932(2)	0.2825(2)	0.2041(2)
O(2)	0.4217(2)	0.1743(2)	0.1070(2)
O(3)	0.5013(2)	0.4048(2)	0.0324(2)
O(4)	0.2786(2)	0.5170(2)	0.1380(2)
C(1)	0.2806(2)	0.3172(2)	0.1628(2)
C(2)	0.3838(2)	0.2674(2)	0.1177(2)
C(3)	0.4176(2)	0.3734(2)	0.0843(2)
C(4)	0.3199(2)	0.4239(2)	0.1305(2)
H(11)	−0.139	0.541	0.168
H(12)	−0.113	0.416	0.000
H(13)	0.141	0.145	0.375
H(21)	−0.193	0.521	0.250
H(22)	0.002	0.354	0.025
H(23)	0.082	0.188	0.438

(H)Yb(H$_2$O)$_6$(C$_4$O$_4$)$_3$ (3(H)-Yb)

The systematic absence of reflections *hkl* with $h+k$ odd and *h0l* with $h+l$ odd was relevant to space groups $C2/c$ and Cc. The structure was refined successfully using $C2/c$. All non-H atoms were refined anisotropically. The water molecules H atoms could be located. In the last cycle of refinement the largest (variable shift)/(e.s.d.) ratio was equal to 0.02 and the reliability factors stabilized at $R = 0.024$ and $R_w = 0.033$ for 2778 observations with $I > 3\sigma(I)$ and 106 variables. The error in an observation of unit weight was 1.11 e. The final difference Fourier map did not show significant features. The atomic coordinates are given in Table 7.

Description and Discussion of the Structures

Pr$_2$(H$_2$O)$_{11}$(C$_4$O$_4$)$_3$·2H$_2$O (1-Pr)

As mentioned in 'Experimental' the structure was determined in space group $P2/c$ and it appeared disordered. There are $Z = 2$ units of formula $[Pr_2(H_2O)_{11}(C_4O_4)_3]\cdot 2H_2O$ per cell: four Pr atoms, four squarate ligands (atoms C(11) to C(41) and O(11) to O(41)), and twenty water molecules are orderly distributed on general positions with full site occupancies. The remaining two squarate entities and six water molecules are disorderly distributed around the twofold axis in a way sketched in Fig. 1. One of the squarate CO bonds crosses the twofold axis so that the two atoms of the bond occupy equivalent positions. In the refinement these positions were attributed to a 'mixed' carbon–oxygen atom named C(O) or O(C) according to the configuration considered. Consequently, the other three CO

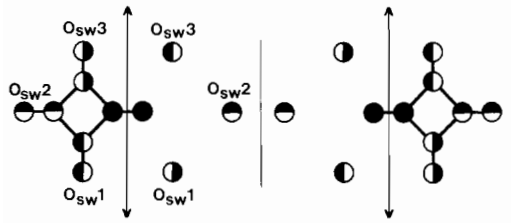

Fig. 1. A sketch illustrating the relation between the disordered squarate anion and three water molecules around the direct twofold axis (represented by the conventional crystallographic symbol). 50% and 100% occupancies are illustrated by half and full black circles, respectively.

TABLE 8. Root-mean-squares displacements (Å) of atoms in 1-Pr

Atom	Min.	Intermediate	Max.
Pr	0.093	0.107	0.159
$O_w(1)$	0.121	0.155	0.210
$O_w(2)$	0.138	0.148	0.200
$O_w(3)$	0.140	0.166	0.271
$O_w(4)$	0.146	0.155	0.199
O_w	0.141	0.147	0.247
O(11)	0.098	0.142	0.273
O(21)	0.099	0.138	0.188
O(31)	0.114	0.143	0.186
O(41)	0.101	0.155	0.269
$O_{sw}(1)$	0.130	0.152	0.223
$O_{sw}(2)$	0.139	0.150	0.295
$O_{sw}(3)$	0.109	0.186	0.280
O(C)	0.130	0.133	0.226
C(1)	0.051	0.127	0.155
C(2)	0.089	0.118	0.149
C(3)	0.096	0.133	0.144
C(11)	0.115	0.120	0.192
C(21)	0.098	0.120	0.151
C(31)	0.112	0.137	0.151
C(41)	0.103	0.121	0.192

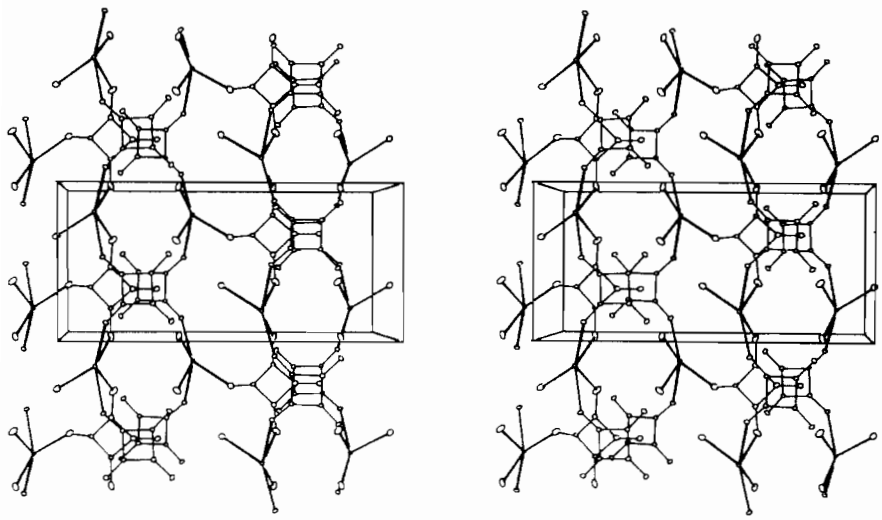

Fig. 2. A stereoview down the *a* axis of the crystal structure of 1-Pr (*b* vertical). A double-chain is indicated by the curved segment. For the sake of clarity, non-disordered water oxygen atoms either coordinated to Pr or non bounded have been omitted.

bonds are on either of the sides of the twofold axis. The three C atoms have 50% site occupancies, while the three O atoms are 50% squarate and 50% water (hence their names: $O_{sw}(1)$, $O_{sw}(2)$, $O_{sw}(3)$). The twofold axis with the subsequent centrosymmetricity is but an artefact resulting from the disorder. The actual structure is not centrosymmetric and the true space group is *Pc* which yields the same systematic extinctions as *P2/c*. It is most surprising that chemically non-equivalent atoms, as are a water oxygen atom and a squarate oxygen atom, occupy positions which, though not rigorously equivalent, are so tightly centrosymmetrically related that the r.m.s. displacement of the single atom which stands for them in the refinement does not show excessive anisotropy compared with that of any ordered oxygen atom (Table 8). The praseodymium is bound to four water molecules and two squarate entities sq(1), and either one squarate entity sq(2) and two water molecules or two squarate entities sq(2) and one water molecule. The two corresponding coordination polyhedra are quite superposable non-regular tricapped trigonal prisms. The presence of two symmetrically independent lanthanide sites per cell was further confirmed by an Eu(III) emission spectroscopy experiment on Eu^{3+}-doped (1-La). The results have been presented elsewhere [1, 10, 11]. Two sites without symmetry were characterized by site selective excitation in the $^5D_2$ sub-levels and time resolved spectroscopy at 77 K. The incidental identity of coordination geometries of both sites results in two sets of very similar energy levels. A question still remains since the two sites do not have equal distribution probabilities as crystallographically required. Further experiments are currently in progress.

Main bond lengths and angles are given in Table 9. The stereoscopic view of the cell content presented in Fig. 2 shows one of the two equally possible Pc configurations. Any ordered squarate anion sq(1) bridges two Pr atoms in a *cis*-bismonodentate mode, while any disordered one sq(2) relates three Pr atoms in a trismonodentate mode. It results in a double chained structure which accommodates two non-coordinating water molecules per unit cell. The double chains run parallel to the *b* axis.

TABLE 9. Interatomic distances (A)[a] and bond angles (°) in $Pr_2(H_2O)_{11}(C_4O_4)_3 \cdot 2H_2O$ (1-Pr)

Around Pr			
Pr–O(11)^{ii}	2.442(4)	Pr–O_w(4)	2.570(3)
Pr–O(21)^{i}	2.412(3)	Pr–O_{sw}(1)	2.568(4)
Pr–O_w(1)	2.481(3)	Pr–O_{sw}(2)	2.576(4)
Pr–O_w(2)	2.598(3)	Pr–O_{sw}(3)	2.522(4)
Pr–O_w(3)	2.491(4)		
Squarate ligands			
Ordered sq(1)			
C(11)–O(11)	1.259(6)	C(11)–C(21)	1.450(6)
C(21)–O(21)	1.240(5)	C(21)–C(31)	1.475(7)
C(31)–O(31)	1.245(5)	C(31)–C(41)	1.470(6)
C(41)–O(41)	1.254(6)	C(41)–C(11)	1.458(6)
O(11)–C(11)–C(41)	136.0(4)	O(31)–C(31)–C(21)	134.5(4)
O(11)–C(11)–C(21)	133.3(4)	O(31)–C(31)–C(41)	136.2(4)
C(21)–C(11)–C(41)	90.6(3)	C(21)–C(31)–C(41)	89.2(3)
O(21)–C(21)–C(11)	134.1(4)	O(41)–C(41)–C(31)	134.9(4)
O(21)–C(21)–C(31)	135.8(4)	O(41)–C(41)–C(11)	135.0(4)
C(11)–C(21)–C(31)	90.1(3)	C(11)–C(41)–C(31)	90.0(3)
Pr^{ii}–O(11)–C(11)	142.1(3)	Pr^{i}–O(21)–C(21)	149.0(3)
Disordered sq(2)			
C(1)–O_{sw}(1)	1.41(1)	C(1)–C(2)	1.47(1)
C(2)–O_{sw}(2)	1.215(9)	C(2)–C(3)	1.48(1)
C(3)–O_{sw}(3)	1.38(1)	C(3)–C(O)	1.55(1)
C(O)–O(C)	1.239(5)	C(O)–C(1)	1.488(9)
O_{sw}(1)–C(1)–C(O)	130.3(6)	O_{sw}(3)–C(3)–C(2)	139.0(7)
O_{sw}(1)–C(1)–C(2)	137.3(7)	O_{sw}(3)–C(3)–C(O)	130.4(6)
C(2)–C(1)–C(O)	92.3(6)	C(2)–C(3)–C(O)	89.1(6)
O_{sw}(2)–C(2)–C(1)	138.6(8)	O(C)–C(O)–C(3)	133.5(5)
O_{sw}(2)–C(2)–C(3)	131.1(8)	O(C)–C(O)–C(1)	138.3(5)
C(1)–C(2)–C(3)	89.4(6)	C(1)–C(O)–C(3)	85.9(5)
Pr^{i}–O_{sw}(1)–C(1)	126.8(4)	Pr^{ii}–O_{sw}(3)–C(3)	125.1(4)
Pr–O_{sw}(2)–C(2)	145.0(5)		

(continued)

TABLE 9. *(continued)*

Hydrogen bonds			
Intramolecular			
$O_w(2)-O(31)^{i}$	2.843(5)	$O_w(2)-H_w(12)-O(31)^{i}$	145.6(3)
$O_w(2)-O(41)^{ii}$	2.722(5)	$O_w(2)-H_w(22)-O(41)^{ii}$	159.5(3)
Intermolecular			
$O_w(1)-O_{sw}(1)$	2.774(5)	$O_w(1)-H_w(11)-O_{sw}(1)$	154.4(3)
$O_w(1)-O_w^{iii}$	2.797(6)	$O_w(1)-H_w(21)-O_w^{iii}$	169.8(3)
$O_w(3)-O(31)^{iii}$	2.806(5)	$O_w(3)-H_w(13)-O(31)^{iii}$	162.2(3)
$O_w(3)-O_w^{iv}$	2.873(6)	$O_w(3)-H_w(23)-O_w^{iv}$	167.9(3)
$O_w(4)-O(31)^{v}$	2.952(5)	$O_w(4)-H_w(14)-O(31)^{v}$	143.7(2)
$O_w(4)-O(41)^{vi}$	2.848(6)	$O_w(4)-H_w(24)-O(41)^{vi}$	150.3(3)
$O_w-O(11)^{ii}$	2.823(5)	$O_w-H_w(1)-O(11)^{ii}$	150.0(3)
$O_w-O(41)^{iii}$	2.784(5)	$O_w-H_w(2)-O(1)^{iii}$	143.2(3)
$O_{sw}(1)-O(C)$	2.625(6)		
$O_{sw}(3)-O(C)$	2.660(6)		

[a]Code of equivalent positions: $^{i} = -x, -y, -z$; $^{ii} = -x, 1-y, -z$; $^{iii} = x, y, \frac{1}{2}-z$; $^{iv} = 1-x, 1-y, -z$; $^{v} = 1+x, -y, z-\frac{1}{2}$; $^{vi} = 1+x, 1-y, z-\frac{1}{2}$.

The squarate ligands stack up following the sequence .....sq(1)-sq(1)-sq(2)..... (Fig. 3). The deviation from planarity of sq(2) will be discussed later. Two neighbouring sq(1) C-cycles slightly overlap with an inter-distance of 3.2 Å. The sq(2) bond C(O)–O(C) is sandwiched between two sq(1) C-cycles from which it is distant of 3.2 Å on the average. Due to the partial double bond character of the bond C(O)–O(C) (1.24 Å) and the aromatic character of the squarate species, these distances are likely to result from some charge-transfer as discussed by Macintyre and Werkema [12].

As the H atoms of the disordered water molecules could not be located, only H bonds involving the ordered water molecules are known (Table 9). Intrachain H-bonds relate the water oxygen atom

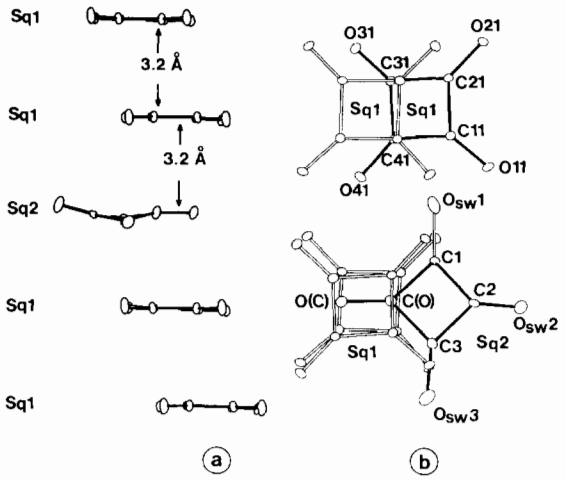

Fig. 3. The stacking of squarate anions, sq(1) and sq(2), in 1-Pr: (a) side view; (b) overlapping schemes of neighboring units.

$O_w(2)$ to the Pr-free squarate oxygen atoms O(31) and O(41), and the water oxygen atom $O_w(1)$ to the mixed atom $O_{sw}(1)$. Interchain H bonds relate O(31) to $O_w(3)$ and $O_w(4)$. The non-coordinated water molecule (oxygen O_w) plays a noticeable cohesive role by being H-bonded both to the squarate O(11) and O(41) atoms of two neighboring chains and to the water molecules w(1) and w(3) of another couple of chains.

$[Eu(H_2O)_4]_2(C_4O_4)_3$ (2-Eu)

There are $Z = 2$ units of formula $[Eu(H_2O)_4]_2(C_4O_4)_3$ per cell and the crystal structure is made of stacked double layers parallel to (100). According to its mean abscissa $x = 0$ or $x = \frac{1}{2}$, a layer contains europium atoms Eu(1) or Eu(2) respectively related to each other by tris-monodentate squarate anions sq(1) or sq(2). Networks of formula $[Eu(1)sq(1)]_{2\infty}$ and $[Eu(2)sq(2)]_{2\infty}$ are thus formed. The association of two such layers by the bis-monodentate squarate anions sq(3) through Eu(1)–sq(3)–Eu(2) bridges give rise to double layers $\{[sq(1)-Eu(1)-]-sq(3)-[-Eu(2)-sq(2)]\}_{2\infty}$. These double layers are separated by van der Waals gaps. All water molecules are bound to europium atoms. A stereoscopic view of the unit cell is given in Fig. 4. Main bond lengths and angles are given in Table 10.

Both Eu(1) and Eu(2) atoms are coordinated by four water and four squarate oxygen atoms with distances varying from 2.300(1) to 2.502(9) Å for Eu(1) and from 2.336(9) to 2.470(7) Å for Eu(2) without any differentiation according to the oxygen origin. In both cases the coordination geometry is close to that of a square antiprism.

The three independent squarate anions show significant deviations from planarity (Fig. 5) along with some unusual bond lengths. These features

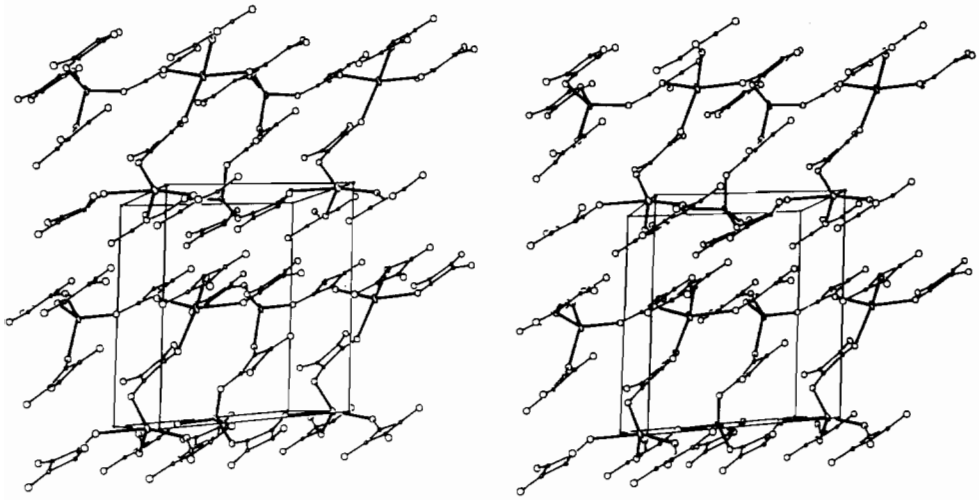

Fig. 4. A stereoview down the *b* axis of the crystal structure of **2**-Eu emphasizing the double-layer structure (*a* vertical). For the sake of clarity water oxygen atoms have been omitted.

TABLE 10. Interatomic distances (Å)[a] and bond angles (°) in $[Eu(H_2O)_4]_2(C_4O_4)_3$ (**2**-Eu)

Around Eu			
Eu(1)–O(11)^{i}	2.42(1)	Eu(2)–O(12)^{i}	2.470(7)
Eu(1)–O(31)^{ii}	2.428(8)	Eu(2)–O(32)^{ii}	2.381(9)
Eu(1)–O(41)^{iii}	2.502(9)	Eu(2)–O(42)	2.395(9)
Eu(1)–O(33)^{iv}	2.30(1)	Eu(2)–O(43)	2.41(2)
Eu(1)–O_w(11)	2.409(9)	Eu(2)–O_w(12)	2.38(1)
Eu(1)–O_w(21)	2.41(1)	Eu(2)–O_w(22)	2.336(9)
Eu(1)–O_w(31)	2.492(8)	Eu(2)–O_w(32)	2.36(1)
Eu(1)–O_w(41)	2.34(2)	Eu(2)–O_w(42)	2.45(1)

Squarate ligands	i = 1	i = 2	i = 3
C(1i)–O(1i)	1.19(1)	1.24(1)	1.27(2)
C(2i)–O(2i)	1.28(1)	1.23(2)	1.24(2)
C(3i)–O(3i)	1.27(1)	1.30(1)	1.44(2)
C(4i)–O(4i)	1.27(1)	1.28(1)	1.21(2)
C(1i)–C(2i)	1.48(1)	1.44(2)	1.54(2)
C(2i)–C(3i)	1.47(2)	1.45(2)	1.36(2)
C(3i)–C(4i)	1.46(2)	1.46(2)	1.46(2)
C(4i)–C(1i)	1.46(2)	1.45(2)	1.44(2)
O(1i)–C(1i)–C(4i)	133(1)	136(1)	143(1)
O(1i)–C(1i)–C(2i)	137(1)	135(1)	129(1)
C(2i)–C(1i)–C(4i)	89.3(8)	89.3(9)	88.5(9)
O(2i)–C(2i)–C(1i)	130.1(9)	132(1)	136(1)
O(2i)–C(2i)–C(3i)	140(1)	136(1)	135(1)
C(1i)–C(2i)–C(3i)	88.5(8)	91.5(8)	87.9(1)
O(3i)–C(3i)–C(2i)	134(1)	130(1)	135(1)
O(3i)–C(3i)–C(4i)	136(1)	138(1)	129(1)
C(2i)–C(3i)–C(4i)	89.8(9)	88.4(9)	95(1)
O(4i)–C(4i)–C(3i)	135(1)	130(1)	140(1)
O(4i)–C(4i)–C(1i)	130(1)	138(1)	132(1)
C(1i)–C(4i)–C(3i)	89.9(9)	90.7(9)	88(1)
Eu(1)^{v}–O(11)–C(11)	138.6(9)	Eu(2)^{v}–O(12)–C(12)	129.7(7)
Eu(1)^{vi}–O(31)–C(31)	133.8(8)	Eu(2)^{vi}–O(32)–C(32)	138.3(8)
Eu(1)^{vii}–O(41)–C(41)	130.3(7)	Eu(2)–O(42)–C(42)	137.0(7)
Eu(1)^{viii}–O(33)–C(33)	132.4(8)	Eu(2)–O(43)–C(43)	142.7(9)

(continued)

TABLE 10. *(continued)*

Hydrogen bonds			
Intra-layer			
$O_w(11)-O(31)^{iii}$	2.64(1)	$O_w(11)-H_w(111)-O(31)^{iii}$	167.9(6)
$O_w(31)-O(41)^{i}$	2.73(1)	$O_w(31)-H_w(131)-O(41)^{i}$	170(1)
$O_w(41)-O(21)^{ii}$	2.76(1)	$O_w(41)-H_w(241)-O(21)^{ii}$	160.3(8)
$O_w(12)-O(22)^{i}$	2.83(1)	$O_w(12)-H_w(212)-O(22)^{i}$	119.8(6)
$O_w(32)-O(42)^{ii}$	2.79(1)	$O_w(32)-H_w(132)-O(42)^{ii}$	152.4(8)
Intra-double-layer			
$O_w(11)-O(23)^{ix}$	2.79(2)	$O_w(11)-H_w(211)-O(23)^{ix}$	151.8(6)
$O_w(42)-O(13)^{x}$	2.43(1)	$O_w(42)-H_w(142)-O(13)^{x}$	161.9(8)
$O_w(21)-O(43)^{iv}$	2.71(1)	$O_w(21)-H_w(221)-O(43)^{iv}$	132.0(7)
Inter-double-layer			
$O_w(41)-O(22)^{iii}$	2.75(1)	$O_w(41)-H_w(141)-O(22)^{iii}$	132.5(7)
$O_w(12)-O(21)$	2.62(1)	$O_w(12)-H_w(112)-O(21)$	156.3(6)

[a]Code of equivalent positions: $^{i} = x, 1-y, z-\frac{1}{2}$; $^{ii} = x, 2-y, z-\frac{1}{2}$; $^{iii} = x, y, z-1$; $^{iv} = x-1, y, z$; $^{v} = x, 1-y, \frac{1}{2}+z$; $^{vi} = x, 2-y, \frac{1}{2}+z$; $^{vii} = x, y, 1+z$; $^{viii} = 1+x, y, z$; $^{ix} = x-1, 1+y, z$; $^{x} = x-1, 1+y, z-1$; $^{xi} = x-1, 1-y, \frac{1}{2}+z$.

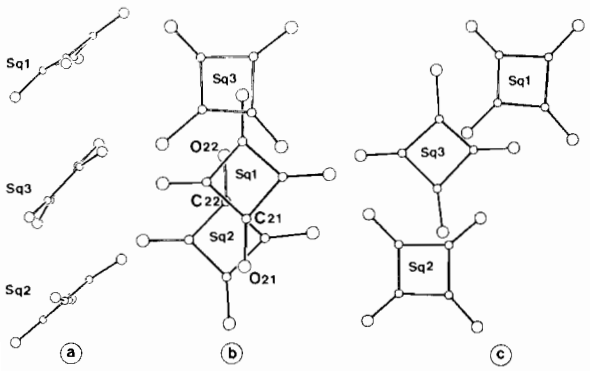

Fig. 5. The stacking of squarate anions, sq(1), sq(2) and sq(3) in **2**-Eu: (a) side view; (b) and (c) overlapping schemes of neighboring units.

will be discussed below. They show a trend to stacking according to the sequence ...sq(1)-sq(2)-sq(3)... (Fig. 5(a)). The mean planes of the sq(1) and sq(2) anions are nearly parallel to each other and they make an angle of about 10° with the mean plane of the sq(3) anion. A projection of the three entities onto the mean planes of the sq(3) C-square shows that there is no overlap between sq(3) and sq(1) or sq(2) entities (Fig. 5(c)). However, a projection onto the mean plane of the sq(2) C-square, for instance, shows a wide overlap of each of the sq(1) and sq(2) C-square by the C(2)–O(2) bond of the facing entity (Fig. 5(b)): atoms C(21) and O(21) are at 3.29 and 3.36 Å from the mean planes of atoms C(12), C(22), C(32), C(42), and atoms C(22) and O(22) are at 3.37 and 3.29 Å from the mean plane of atoms C(11), C(21), C(31), C(41). Such distances between the π-systems of the CO bond and of the C-square are indicative of a van der Waals interaction that takes place in the inter-double-layer gap. It is the only noticeable van der Waals interaction of the structure. The cohesion between double layers is strengthened by H bonds from water molecules w(41) and w(12) to europium-free squarate oxygen atoms O(22) and O(21), respectively (Table 10). Intralayer hydrogen bonds are also present (Table 10).

Europium emission spectroscopy at 77 K gave two informations [1, 10]. First, it confirmed the presence of two non-identical europium sites, with again the puzzling unequality of distribution probabilities that was mentioned above for (**1**-La). Secondly, a broad strong UV emission band (around 19 000 cm^{-1}) characteristic of the allowed Eu^{2+} $4f^n \rightarrow 4f^{n-1}$ transition was observed. Therefore, the unexpected yellow coloration of **2**-Eu (and by the way of **2**(H)-Eu) is due to a trace of Eu(II) species.

$Eu(H_2O)_6(C_4O_4)(HC_4O_4)\cdot H_2O$ (2(H)-Eu)

The C-centered unit cell contains four units of formula $Eu(H_2O)_6(C_4O_4)(HC_4O_4)\cdot H_2O$. A view of a unit is given in Fig. 6. Main interatomic distances and bond angles are listed in Table 11. The

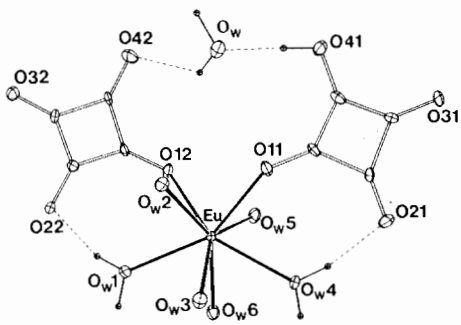

Fig. 6. A drawing of the $Eu(H_2O)_6(C_4O_4)(HC_4O_4)$ unit in **2**(H)-Eu. H atoms of molecules not involved in H-bonding have been omitted.

TABLE 11. Interatomic distances (Å)[a] and bond angles (°) in $Eu(H_2O)_6(C_4O_4)(HC_4O_4)\cdot H_2O$ (2(H)-Eu)

Around Eu			
Eu–O(11)	2.307(3)	Eu–O_w(3)	2.396(3)
Eu–O(12)	2.383(3)	Eu–O_w(4)	2.427(3)
Eu–O_w(1)	2.382(3)	Eu–O_w(5)	2.425(3)
Eu–O_w(2)	2.493(3)	Eu–O_w(6)	2.431(3)
Monohydrogenosquarate			
C(11)–O(11)	1.248(4)	C(11)–C(21)	1.501(5)
C(21)–O(21)	1.227(5)	C(21)–C(31)	1.515(5)
C(31)–O(31)	1.248(4)	C(31)–C(41)	1.417(5)
C(41)–O(41)	1.296(5)	C(41)–C(11)	1.438(5)
O(11)–C(11)–C(41)	136.0(3)	O(31)–C(31)–C(21)	134.1(3)
O(11)–C(11)–C(21)	134.3(3)	O(31)–C(31)–C(41)	136.0(3)
C(21)–C(11)–C(41)	89.6(3)	C(21)–C(31)–C(41)	89.8(3)
O(21)–C(21)–C(11)	134.4(3)	O(41)–C(41)–C(31)	131.0(3)
O(21)–C(21)–C(31)	138.5(3)	O(41)–C(41)–C(11)	135.5(4)
C(11)–C(21)–C(31)	87.1(3)	C(11)–C(41)–C(31)	93.4(3)
		Eu–O(11)–C(11)	146.4(3)
Squarate			
C(12)–O(12)	1.271(4)	C(12)–C(22)	1.423(5)
C(22)–O(22)	1.263(4)	C(22)–C(32)	1.433(5)
C(32)–O(32)	1.259(4)	C(32)–C(42)	1.490(4)
C(42)–O(42)	1.251(5)	C(42)–C(12)	1.456(5)
O(12)–C(12)–C(42)	132.6(3)	O(32)–C(32)–C(22)	138.3(3)
O(12)–C(12)–C(22)	136.4(3)	O(32)–C(32)–C(42)	132.3(3)
C(22)–C(12)–C(42)	91.0(2)	C(22)–C(32)–C(42)	89.2(3)
O(22)–C(22)–C(12)	135.5(3)	O(42)–C(42)–C(32)	136.1(3)
O(22)–C(22)–C(32)	132.9(3)	O(42)–C(42)–C(12)	135.8(3)
C(12)–C(22)–C(32)	91.6(3)	C(12)–C(42)–C(32)	88.0(3)
		Eu–O(12)–C(12)	136.5(2)
Hydrogen bonds			
Intramolecular			
O(41)–O_w	2.525(5)	O(41)–H(41)–O_w	143.3(3)
O_w–O(42)	2.989(6)	O_w–H_w(2)–O(42)	128.0(3)
O_w(1)–O(22)	2.664(4)	O_w(1)–H_w(21)–O(22)	161.1(2)
O_w(4)–O(21)	2.737(4)	O_w(1)–H_w(24)–O(21)	168.3(2)
Intermolecular			
O_w–$O(12)^{i}$	2.737(5)	O_w–H_w(1)–$O(12)^{i}$	173.0(2)
O_w(1)–$O(31)^{ii}$	2.797(4)	O_w(1)–H_w(11)–$O(31)^{ii}$	160.9(2)
O_w(2)–$O(21)^{iii}$	2.673(5)	O_w(2)–H_w(12)–$O(21)^{iii}$	152.6(2)
O_w(2)–$O(42)^{i}$	2.881(4)	O_w(2)–H_w(22)–$O(42)^{i}$	149.2(2)
O_w(3)–$O(6)^{iv}$	3.028(4)	O_w(3)–H_w(13)–$O_w(6)^{iv}$	114.3(2)
		O_w(3)–H_w(23)–$O_w(6)^{iv}$	119.5(2)
O_w(3)–$O(32)^{v}$	2.868(4)	O_w(3)–H_w(13)–$O(32)^{v}$	132.0(2)
O_w(3)–$O(31)^{iii}$	2.814(4)	O_w(3)–H_w(23)–$O(31)^{iii}$	154.6(2)
O_w(4)–$O(32)^{vi}$	2.771(4)	O_w(4)–H_w(14)–$O(32)^{vi}$	162.3(2)
O_w(5)–$O(22)^{vii}$	2.621(5)	O_w(5)–H_w(15)–$O_w(22)^{vii}$	171.9(2)
O_w(5)–$O_w(2)^{viii}$	2.962(5)	O_w(5)–H_w(25)–$O_w(2)^{viii}$	151.4(2)
O_w(5)–O_w^{ix}	3.093(5)	O_w(5)–H_w(25)–O_w^{ix}	114.7(2)
O_w(6)–O(32)	2.857(4)	O_w(6)–H_w(16)–O(32)	138.0(3)
O_w(6)–$O(31)^{x}$	2.962(5)	O_w(6)–H_w(26)–$O_w(31)^{x}$	164.8(2)

[a]Code of equivalent positions; $^{i} = x, 1-y, z-\frac{1}{2}$; $^{ii} = x-\frac{1}{2}, \frac{1}{2}+y, z$; $^{iii} = x-\frac{1}{2}, -y-\frac{1}{2}, z-\frac{1}{2}$; $^{iv} = x, 2-y, z-\frac{1}{2}$; $^{v} = \frac{1}{2}+x, \frac{3}{2}-y, z-\frac{1}{2}$; $^{vi} = \frac{1}{2}+x, \frac{1}{2}+y, z$; $^{vii} = \frac{1}{2}+x, \frac{3}{2}-y, \frac{1}{2}+z$; $^{viii} = x, y, 1+z$; $^{ix} = x, 1-y, \frac{1}{2}+z$; $^{x} = x-\frac{1}{2}, \frac{3}{2}-y, \frac{1}{2}+z$.

Eu atom is bound to six water molecules and two monodentate squarate ligands. The polyhedron of coordination is close to a bicapped trigonal prism. One of the squarate ligands appeared to be monohydrogenated. The unique non-coordinated water molecule bridges the two squarate ligands through two H bonds involving its atom H(2) and the squarate H atom. The water molecules w(1) and w(4) are H-bound to their adjacent squarate O atoms, O(22) and O(21), respectively. The whole molecular unit contains three adjacent rings (Fig. 6).

The salient feature of this structure is the presence of both a squarate anion and a hydrogenosquarate anion as ligands. The hydroxyl function of the hydrogenosquarate species is at O(41) and consistently the largest C–O bond is C(41)–O(41) = 1.296(5) Å. The C–C and C–O bond length distribution displays a pseudo twofold symmetry around the diagonal C(41)–C(21) segment: in a *trans* position to the largest C–O bond stands the shortest one (C(21)–O(21) = 1.227(5) Å), while the two other ones, C(11)–O(11) and C(31)–O(31) are intermediate, equal to 1.248(4) Å. Adjacent to the shortest C–O bonds are the largest C–C ones: C(21)–C(11) = 1.501(5) Å and C(21)–C(31) = 1.515(5) Å; adjacent to the largest C–O bond are the shortest C–C ones: C(41)–C(11) = 1.438(5) Å and C(41)–C(31) = 1.417(5) Å. The distribution of bond lengths and angles fits quite well that found in $M(H_2O)_6(HC_4O_4)_2 \cdot 2H_2O$ (M = Ni, Co) [13] and in $M(HC_4O_4)$ (M = Na, K) [14] as shown in Table 12.

TABLE 12. Compared geometries of $[HC_4O_4]^-$ anions in 2(H)-Eu and in some known structures (references in text)

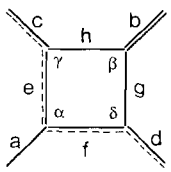

	2(H)-Eu	$M(H_2O)_6(HC_4O_4)_2 \cdot 2H_2O$		$M(HC_4O_4)$	
		M = Ni	M = Co	M = Na	M = K
a	1.296(5)	1.308(1)	1.310(2)	1.306(5)	1.295(5)
b	1.227(5)	1.239(4)	1.238(3)	1.218(5)	1.235(4)
c	1.248(4)	1.240(1)	1.246(1)	1.264(4)	1.277(4)
d	1.248(4)	1.235(1)	1.238(2)	1.241(4)	1.245(4)
e	1.438(5)	1.438(1)	1.437(3)	1.421(5)	1.415(4)
f	1.417(5)	1.439(1)	1.444(3)	1.435(5)	1.458(5)
g	1.515(5)	1.481(1)	1.481(1)	1.503(5)	1.500(4)
h	1.501(5)	1.479(1)	1.484(1)	1.498(4)	1.477(5)
α	93.4(3)	93.2(1)	93.2(2)	93.2(3)	93.2(3)
β	87.1(3)	89.9(9)	89.8(2)	87.5(3)	89.1(3)
γ	89.6(3)	88.5(7)	88.6(1)	90.0(3)	90.1(3)
δ	89.8(3)	88.4(7)	88.4(1)	89.3(3)	87.6(3)

(H)Yb(H₂O)₆(C₄O₄)₃ (3(H)-Yb)

The atoms located through the structure determination form discrete anionic entities (Fig. 7) having the formula $[Yb(H_2O)_6(C_4O_4)_2]^-$. There are four such entities per C-centered unit cell. The H^+ counterions needed for the sake of electroneutrality could not be located in the course of the structure refinement. However they are most likely to occupy the inversion centres 4(a) or random positions nearby, as will be shown. Interatomic distances and bond angles are listed in Table 13.

The Yb atoms occupy the 4(e) special positions in space group $C2/c$. Therefore a $Yb(H_2O)_6(C_4O_4)_2$ unit has the crystallographically imposed point symmetry 2. Each Yb atom is bound to two monodentate squarate oxygen atoms (2 × O(1)) at 2.369(2) Å and six water oxygen atoms (2 × $O_w(1)$, $O_w(2)$, $O_w(3)$) at shorter distances, 2.315(2), 2.328(2) and 2.280(2) Å, respectively. The coordination geometry is closely related to that of a square antiprism. There is an intramolecular H bond between the water oxygen $O_w(1)$ and the squarate oxygen O(4).

A screening of the interanionic distances revealed a contact of 2.487(3) Å between nearby squarate oxygen atoms O(3). This distance is too short to stem from a simple van der Waals interaction, but it is well in the domain of the short O–H–O bonds (O···O < 2.55 Å) [15]. As atoms O(3) are centrosymmetrically related, the protons might well be located at the relevant centres of inversion, i.e. (0, 0, 0), (0, 0, $\frac{1}{2}$), ($\frac{1}{2}$, $\frac{1}{2}$, 0), ($\frac{1}{2}$, $\frac{1}{2}$, $\frac{1}{2}$). However there is no definite proof about the symmetry of this bond, and the protons might as well be randomly distributed in positions close to the centres of inversion. Infrared spectroscopy is of no help since unsymmetrical H bonds also occur between water molecules and squarate ligand (Table 13).

A further indirect proof of the presence of protons within the O(3)···O(3) intervals is the significant lengthening by *c.* 0.03–0.04 Å of the bond C(3)–O(3) measuring 1.279(3) Å, with respect to the other three C–O bonds measuring 1.239(3), 1.244(3) and 1.248(3) Å.

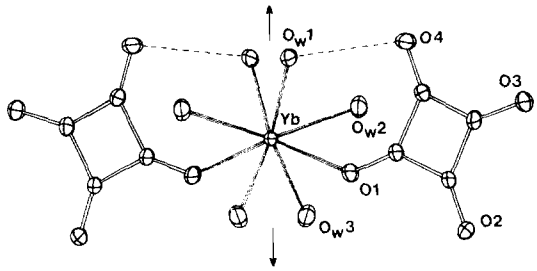

Fig. 7. A drawing of the $[Yb(H_2O)_6(C_4O_4)_2]^-$ unit in 3(H)-Yb. The direct twofold axis is represented by the conventional crystallographic symbol.

TABLE 13. Interatomic distances (Å)[a] and bond angles (°) in $H[Yb(H_2O)_6(C_4O_4)_2]$ (3(H)-Yb)

Around Yb					
Yb–O(1)[O(1)^{i}]	2.369(2)	Yb–O_w(2)[O_w(2)^{i}]	2.328(2)		
Yb–O_w(1)[O_w(1)^{i}]	2.315(2)	Yb–O_w(3)[O_w(3)^{i}]	2.280(2)		
Squarate					
C(1)–O(1)	1.239(3)	O(1)–C(1)–C(4)	135.7(2)	O(3)–C(3)–C(2)	132.2(2)
C(2)–O(2)	1.243(3)	O(1)–C(1)–C(2)	134.9(2)	O(3)–C(3)–C(4)	136.1(2)
C(3)–O(3)	1.279(3)	C(2)–C(1)–C(4)	89.3(2)	C(2)–C(3)–C(4)	91.7(2)
C(4)–O(4)	1.248(3)	O(2)–C(2)–C(1)	135.7(2)	O(4)–C(4)–C(3)	136.9(2)
C(1)–C(2)	1.479(3)	O(2)–C(2)–C(3)	134.9(2)	O(4)–C(4)–C(1)	133.3(2)
C(2)–C(3)	1.453(3)	C(1)–C(2)–C(3)	89.3(2)	C(1)–C(4)–C(3)	89.7(2)
C(3)–C(4)	1.444(4)				
C(4)–C(1)	1.477(3)	Yb–O(1)–C(1)	139.1(2)		
Hydrogen bonds					
Intramolecular					
O_w(1)–O(4)^{i}	2.673(3)	O_w(1)–H_w(21)–O(4)^{i}	153.6(1)		
Intermolecular					
O(3)–O(3)^{ii}	2.487(3)	H not located (see text)			
O_w(1)–O(2)^{iii}	2.754(3)	O_w(1)–H_w(11)–O(2)^{iii}	169.8(1)		
O_w(2)–O(4)^{iv}	2.873(2)	O_w(2)–H_w(12)–O(4)^{iv}	167.2(2)		
O_w(2)–O(2)^{v}	2.705(3)	O_w(2)–H_w(22)–O(2)^{v}	141.9(1)		
O_w(3)–O(3)^{vi}	2.754(4)	O_w(3)–H_w(23)–O(3)^{vi}	154.7(2)		
O_w(3)–O(4)^{vii}	2.695(3)	O_w(3)–H_w(13)–O(4)^{vii}	176.0(1)		

[a]Code of equivalent positions: $^{i} = -x, y, \frac{1}{2} - z$; $^{ii} = 1 - x, 1 - y, -z$; $^{iii} = x - \frac{1}{2}, \frac{1}{2} + y, z$; $^{iv} = -x, 1 - y, -z$; $^{v} = \frac{1}{2} - x, \frac{1}{2} - y, -z$; $^{vi} = x - \frac{1}{2}, \frac{1}{2} - y, \frac{1}{2} + z$; $^{vii} = \frac{1}{2} - x, y - \frac{1}{2}, \frac{1}{2} - z$.

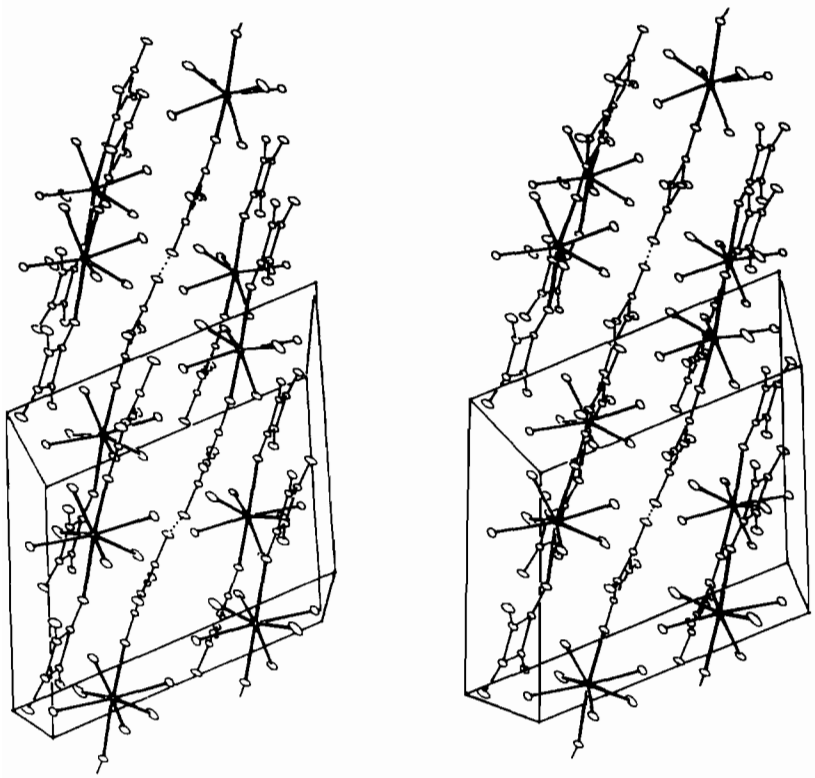

Fig. 8. A stereoview down the *b* axis of the crystal structure of 3(H)-Yb (*a* vertical) showing chaining through intermolecular H-bonding (dotted lines).

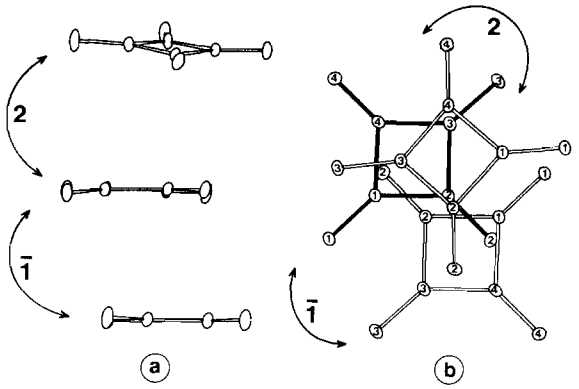

Fig. 9. The stacking of the squarate anion in 3(H)-Yb: (a) side view; (b) overlapping scheme. The operations of symmetry relating the units are indicated by conventional crystallographic symbols.

The short O(3)–H–O(3) bonds link the anions into polymeric chains parallel to the [20$\bar{1}$] row. This is shown on the stereoscopic view of Fig. 8. Interchain H bonds involving water molecules and squarate oxygen atoms O(2), O(3), O(4) are also present. They are listed in Table 13.

The squarate anion is planar, with atom-to-mean-plane distances not exceeding 0.05 Å. It generates stacks by repeating through alternating inversion centres and twofold axes. Two squarate anions related by inversion slightly overlap with a distance of 3.05 Å between mean planes (Fig. 9): the bonds C(2)–O(2) cross the facing bonds C(1)–C(2), so that the O(2) atoms stand above the facing bonds C(1)–C(4) at 3.12 Å from the C-square mean planes. Two squarate anions related by a twofold axis make an angle of 9.4(7)°, and show a wide C-square overlap (Fig. 9): the distances of C(2) and C(4) to the mean plane of the facing C-square are 3.18 and 3.42 Å, respectively. Adjacent bonds C(1)–C(2) and C(1)–C(4) are larger than the corresponding C(3)–C(2) and C(3)–C(4) (1.479(3) and 1.477(3) against 1.444(4) and 1.453(3) Å, respectively) which is consistent with the fact that the first one is flanked by the bonds C(2)–C(3) and C(2)–O(2), the second one by the atom O(2) and the bond C(3)–O(3), while the other two have no close π-interacting neighbours.

The Squarate Anions

In three of the seven squarate ligands encountered in this study (2 in **1**-Pr, 4 in **2**-Eu and **2**(H)-Eu and 1 in **3**(H)-Yb), the carbon square cycle shows a noticeable 'tetrahedral' distortion. The distortion can be evaluated by means of a dihedral angle criterion, by comparing the observed dihedral angles α and β, as defined in Table 12, to those of the regular square and tetrahedral limit symmetries.

When going from the square to the tetrahedron, both α angles vary from 0 to 109.5°, and the four β angles from 180 to 109.5°. The tetrahedral distortion Δ can be evaluated using the following weighted formula

$$\Delta = 0.14[720 - (\beta_1 + \beta_2 + \beta_3 + \beta_4)]/70.5 + 0.22[\alpha_1 + \alpha_2]/109.5$$

The measured dihedral angles and calculated corresponding distortions Δ for the seven squarate ligands are listed in Table 14.

It is possible to relate the presence or absence of distortion to interactions exerted by neighbouring atoms or molecules at the squarate C–O bonds either directly or through the oxygen atoms. The squarate ligand in **2**(H)-Eu and in **3**(H)-Yb and the non-disordered one in **1**-Pr do not show noticeable distortion of their C-squares. The directions

TABLE 14. Dihedral angles and distortions of the squarate C-squares

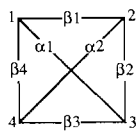

	1-Pr		2-Eu			2(H)-Eu	3(H)-Yb
	sq(1)	sq(2)	sq(1)	sq(2)	sq(3)		
α1	1.3	19.1	16.9	3.3	7.3	4.3	1.9
α2	1.3	19.6	17.0	3.2	7.5	4.3	1.3
β1	179.1	166.4	168.1	177.7	174.8	176.9	178.7
β2	179.1	165.8	168.1	177.7	174.8	176.9	178.7
β3	179.1	166.6	167.9	177.7	174.5	177.0	178.7
β4	179.1	166.4	168.0	177.7	175.1	177.0	178.1
Δ	0.01	0.19	0.16	0.03	0.07	0.04	0.02

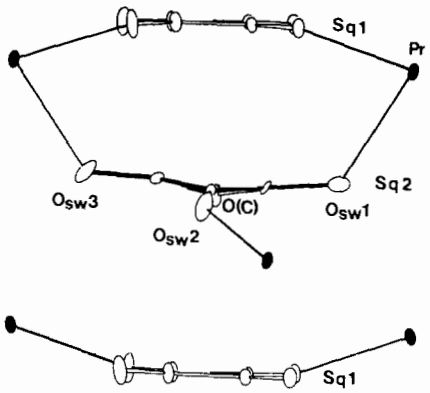

Fig. 10. An illustration of the constraints exerted by Pr atoms on the squarate anion sq(2) in 1-Pr. This view deduces from that of Fig. 3(a) by a 90° rotation around the stacking axis.

of the forces exerted at the squarate O atoms by both the Ln(III) cations and the water molecules are little inclined to the anion mean planes and not compatible with a tetrahedral distortion anyway.

For the other four squarate anions, the Ln(III) cations are quite far out of the anion planes, and the directions of the forces exerted at the squarate O atoms are compatible with a tetrahedral distortion of the C-squares. This is markedly the case for the squarate sq(1) in 1-Pr which exhibits the most deformed C-square with $\Delta = 19\%$. Its situation is depicted in Fig. 10. The C(O)–O(C) bond is clamped as in a vice by two adjacent sq(1) anions (Fig. 3(b)) and its oxygen O(C) is back-anchored to water molecules w(1) and w(3) by intermolecular interactions (not shown on either Fig. 3 or Fig. 10), possibly H bonds or at least van der Waals contacts ($O_{sw}(1)$–O(C) = 2.625(6) Å, $O_{sw}(3)$–O(C) = 2.660(6) Å; H positions are not known). At the opposite corner, the oxygen atom of the C(2)–$O_{sw}(2)$ bond is also back-anchored by a Pr(III) cation at 2.576(4) Å so that the angle C(2)–$O_{sw}(2)$–Pr is nearly straight (145.1(5)°). Meanwhile, two Pr(III) cations strain at the other two oxygen atoms $O_{sw}(1)$ and $O_{sw}(3)$: they stand on the same side of the anion – hence the tetrahedral deformation – and as they are unusually far above the C-square mean plane (2.00 and 2.45 Å respectively) – hence the importance of the force perpendicular components.

A fairly similar situation is met in 2-Eu (Fig. 11) for the anions sq(1) and sq(2) in which three oxygen atoms are bound to three Eu(III) cations standing markedly out of the C-square mean planes (one distance is 0.91 Å while the others range from 1.30 to 1.42 Å) and acting out in such a way as to favour a tetrahedral distortion of the C-square. As outlined above, any C(2*i*)–O(2*i*) bond ($i = 1$ or 2) overlaps the square of the neighboring sq(*j*) squarate

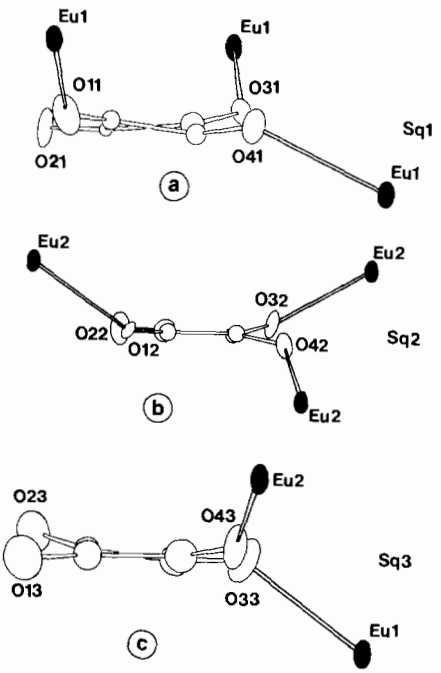

Fig. 11. An illustration of the constraints exerted by Eu atoms on the squarate anions, (a) sq(1), (b) sq(2), (c) sq(3) in 2-Eu.

(*j* = 2 or 1) (Fig. 5(b)) and the mean distance of 3.3 Å is indicative of interacting π-systems. Besides, the O(2*i*) atoms are bound to water molecules w(12) for O(21) and w(41) for O(22). The vertical components of both the H bond and the interaction exerted by the overlapping C-square have the same direction as the vertical component of the attraction of the Eu(III) cation on the opposite oxygen atom O(4*i*) ($i = 1$ or 2). Eu–O(1*i*) and Eu–O(3*i*) bonds act in the reverse direction, as illustrated in Fig. 11. The resulting tetrahedral distortion is marked for sq(1) ($\Delta = 16\%$) but weak if significant for sq(2) ($\Delta = 3\%$). That the two anions do not answer similarly to what looks like quite similar constraints suggests that we are in the presence of borderline constraints and that a more detailed investigation would be necessary to detect which other minor forces turn the balance. The third squarate, sq(3), in 2-Eu has a distortion of 7%. The situation cannot be compared with the previous ones since the anion is bound to only two cations which exert a tearing action by pulling on two adjacent oxygen atoms (Fig. 11).

The non-distorted squarate anions do not show unusual C–C and C–O bond lengths ($1.44 < C–C < 1.48$; $1.23 < C–O < 1.30$), while some unusual values are observed in the distorted ones: one C–C single bond length is observed in the 19% and 7% deformed ligands: 1.55(1) and 1.54(2) Å, respectively. The former is concomitant with two rather

large C–O bonds (1.41(2) and 1.38(2) Å), the latter with one large C–O bond (1.44(2) Å) and one short C–C bond (1.36(2) Å). The 16% deformed ligand exhibits usual C–C and C–O distances except one very short C–O bond of 1.19(1) Å.

Thermal Behaviour

Thermal gravimetry analyses (TGA) and thermal differential analyses (TDA) of compounds of the five families **1**-Ln, **2**-Ln, **1**(H)-Ln, **2**(H)-Ln, **3**(H)-Ln were performed in the temperature range 20–800 °C, in a 50% helium–50% oxygen gas stream. TGA and TDA curves of compounds of families **1**-Ln, **2**-Ln, **1**(H)-Ln and **2**(H)-Ln are presented in Figs. 12, 13, 14 and 15, respectively. For the **3**(H)-Ln family, thermal analyses were done on the Yb derivative; both the TGA and TDA curves look like those of **1**(H)-Ln compounds.

All compounds lose weight in two main steps: complete dehydration followed by decomposition of the anhydrous squarate leaving the suitable oxide. Dehydration takes place in one or two steps. In the latter case, TDA shows two endothermic peaks, but the corresponding partially dehydrated compound is only indicated by a point of inflection on the TGA curve and is therefore hardly isolable. Plateaux corresponding to anhydrous compounds extend over a temperature range about 100 to 300 °C wide. Therefore, anhydrous lanthanide squarates, either protoned or not, are easily isolated. This is a salient feature of lanthanide squarates with respect to oxalates that cannot be isolated in the anhydrous

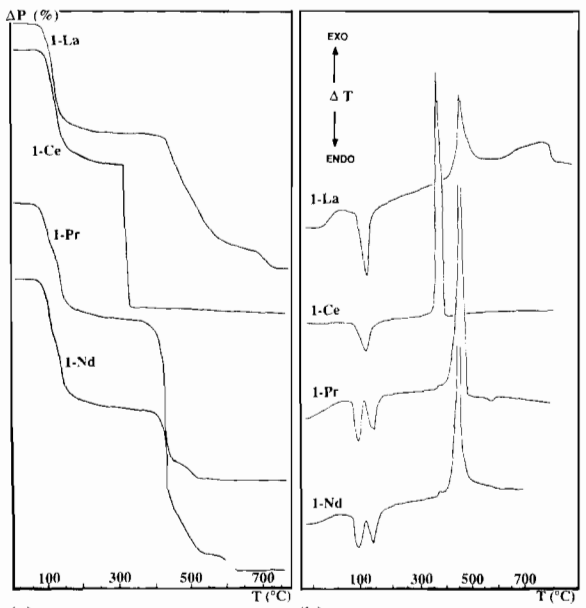

(a) (b)

Fig. 12. TGA (a) and TDA (b) curves for **1**-Ln compounds.

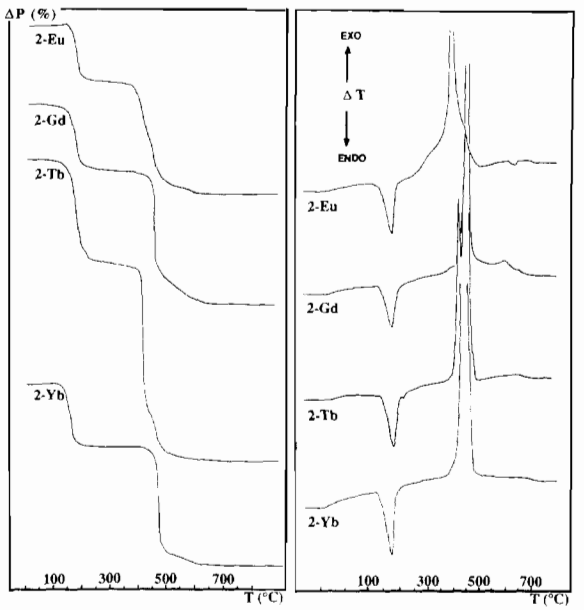

(a) (b)

Fig. 13. TGA (a) and TDA (b) curves for **2**-Ln compounds.

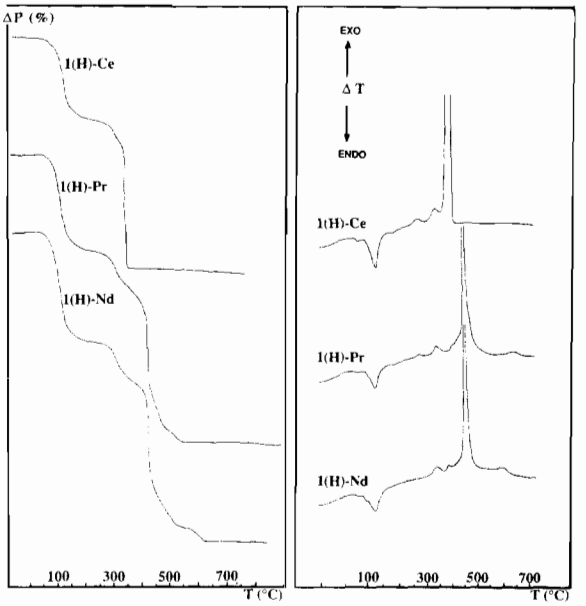

(a) (b)

Fig. 14. TGA (a) and TDA (b) curves for **1**(H)-Ln compounds.

state since oxalate decomposition starts in the dehydration tail [16].

The decomposition of anhydrous squarates of **1**-Ln and **2**-Ln families that are not protonated is a two or even three step process except for **1**-Ce. The corresponding TDA curves show only one major exothermic peak with a minor satellite (except **2**-Tb) or shoulder. The one step, steep slope mode of decomposition of the anhydrous **1**-Ce is also a

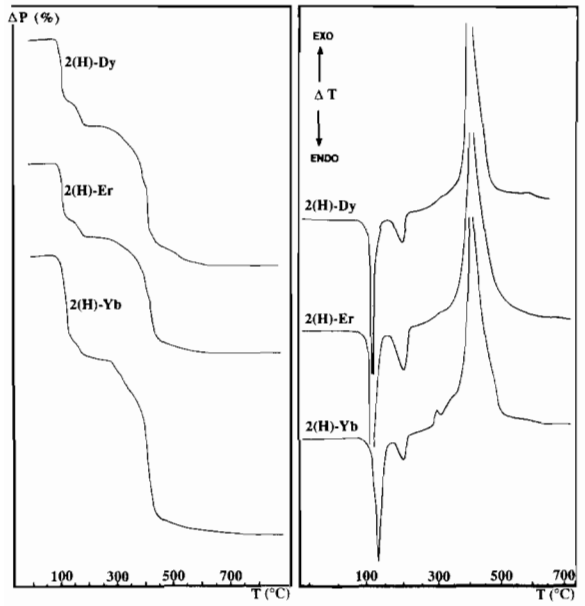

(a) (b)

Fig. 15 TGA (a) and TDA (b) curves for 2(H)-Ln compounds.

feature of the decomposition of the Ce(III) oxalate under oxygen [17–19]. In either case, the final product is the Ce(IV) oxide, CeO_2. The strongly exothermic Ce(III) to Ce(IV) oxidation is most likely to hasten the decomposition process which takes place over a temperature range only 10 °C wide. The corresponding TDA peak exhibits a shoulder. Formation of Ln(IV) occurs also, but partially, with Pr and Tb derivatives that give mixed valence oxides Pr_4O_{11} and Tb_4O_7. The corresponding TGA curves are among the steepest ones and the TDAs show either a broad peak (Pr) or two peaks (Tb). As to the 2-Eu TDA exothermic peak, its broad shouldered foot could result from a three step process similar to the one proposed by Glasner *et al.* [20] and later by Shyamala *et al.* [21] for the thermal decomposition of Eu(III) oxalate in air; reduction of $Eu_2(C_4O_4)_3$ to $Eu(C_4O_4)_2$, decomposition of squarate and Eu(II) to Eu(III) oxidation by air.

The formation of oxocarbonates is another feature in common with the decomposition of oxalates. Here, La(III), Pr(III) and Nd(III) oxocarbonates were isolated. Their IR spectra corresponded to those of dioxomonocarbonates $Ln_2O_2CO_3$ studied by Turcotte *et al.* [19]: $Pr_2O_2CO_3$ and $Nd_2O_2CO_3$ were found of types I and IA, respectively, and $La_2O_2CO_3$ was found as a mixture of types I, IA and II according to Turcotte's nomenclature.

Decomposition of members of the anhydrous protonated families 1(H)-Ln, 2(H)-Ln and 3(H)-Ln begins with the elimination of two protons as water and one squarate as carbon dioxide per couple of lanthanide cations

$$2HLn(C_4O_4)_2 + O_2 = H_2O + 4CO_2 + Ln_2(C_4O_4)_3$$

Then decomposition of anhydrous squarates occurs, as previously described.

Comparison of our results with those of Brzyska and Ozga [5] is hardly possible. In view of their Ln/squarate ratios of 2/3, their compounds are to be compared with those of families 1-Ln and 2-Ln in our nomenclature. The stoichiometries are identical for the La, Ce and Pr derivatives, i.e. three quarters of the 1-Ln family as obtained under our procedure A. Similarity is also observed for the Eu derivative, our 2-Eu compound. All other Brzyska and Ozga's compounds are more hydrated than ours, up to more than three times more in the case of dysprosium. Differences in preparation could possibly account for these discrepancies. However, the great number of structural phases these authors have found (7 according to the different water contents), with no straight relation to the lanthanide contraction, does not fit the usual image of homologous lanthanide compounds that quite often present two or three structural types closely related to the cationic radius continuous variation. Then the question arises as to whether they have worked on pure phases.

Acknowledgements

Financial support by Rhône-Poulenc (Division Minérale Fine) and C.N.R.S. is gratefully acknowledged.

References

1 J.-F. Petit, *Thèse de Doctorat de l'Université,* Université Paul Sabatier, Toulouse, 1988. Presented in part at the poster session of *2nd Int. Conf. Basic and Applied Chemistry of f-Transition and Related Elements (2nd. I.C.L.A.), Lisboa, Portugal, 1987.*
2 E. Orebaugh and G. H. Choppin, *J. Coord. Chem., 5* (1976) 123.
3 A. T. Kandil, N. Souka and K. Farah, *J. Radioanal. Chem., 49* (1979) 13.
4 W. Brzyska and W. Ozga, *Polish J. Chem., 61* (1987) 323.
5 W. Brzyska and W. Ozga, *J. Thermal Anal., 32* (1987) 2001.
6 J.-C. Trombe, J.-F. Petit and A. Gleizes, *Inorg. Chim. Acta, 167* (1990)
7 *SDP Structure Determination Package,* Enraf-Nonius, Delft, 1979; C. K. Johnson, *ORTEP,* a Fortran thermal-ellipsoid plot program for crystal structure illustrations, *Report ORNL-3794,* Oak Ridge National Laboratory, TN, 1965.
8 *International Tables for X-ray Crystallography,* Vol. 4, Kynoch Press, Birmingham, 1974, Tables 2.2A and 2.3.1.
9 A. Mosset, J. J. Bonnet and J. Galy, *Acta Crystallogr., Sect. B, 33* (1977) 2633.

10 B. Piriou, A. Gleizes, J.-F. Petit and J.-C. Trombe, *3ème Congrès National de la Société Française de Chimie (Colloque 2), Nice, France, 1988*; J.-F. Petit, J.-C. Trombe, A. Gleizes and B. Piriou, *26th Int. Conf. Coordination Chemistry (Section A), Porto, Portugal, 1988.*
11 B. Piriou, J.-F. Petit, J.-C. Trombe and A. Gleizes, *J. Chim. Phys., 86* (1989) 1207.
12 W. M. Macintyre and M. S. Werkema, *J. Chem. Phys., 42* (1964) 3563.
13 I. Brach and J. Roziere, B. Anselment and K. Peters, *Acta Crystallogr., Sect. C, 43* (1987) 458.
14 K. Peters, E. M. Peters, H. G. von Schnering and B. Klaholz, personal communication.
15 A. F. Wells, *Structural Inorganic Chemistry*, Clarendon Press, Oxford, 4th edn., 1975, p. 301.
16 P. Pascal, *Nouveau Traité de Chimie Minérale*, Tome VII-2, Masson, Paris, 1959, p. 1006.
17 A. Glasner and M. Steinberg, *J. Inorg. Nucl. Chem., 16* (1961) 279.
18 V. V. Subba Rao, R. V. G. Rao and A. B. Biswas, *J. Inorg. Nucl. Chem., 27* (1965) 2525.
19 R. P. Turcotte, J. O. Sawyer and L. Eyring, *Inorg. Chem., 8* (1969) 238.
20 A. Glasner, E. Levy and M. Steinberg, *J. Inorg. Nucl. Chem., 25* (1963) 1415.
21 M. Shyamala, S. R. Dharwadkar and M. S. Chandrasek-Haraiah, *Thermochim. Acta, 56* (1982) 135.